 DOI: 10.1002/masy.201200016

Synthesis and Electron Transfer Properties of Metal Complex Oligomer Wires with an Inherent Potential Gradient on Gold Electrode

*Yoshihiko Nishimori, Hiroaki Maeda, Shunsuke Katagiri, Junya Sendo, Mariko Miyachi, Ryota Sakamoto, Yoshinori Yamanoi, Hiroshi Nishihara**

Summary: π-Conjugated bis(terpyridine)metal ($M(tpy)_2$) oligomer wires were prepared by surface coordination programming such that they displayed an inherent potential gradient along the wire through the chain of metals and bridging ligands. The electron transfer properties of these wires were examined. Heterometal complex wires prepared in the sequence Au(111)-$Co(tpy)_2$-$Fe(tpy)_2$-ferrocene (Fc); that is, Au-[$\mathbf{A_{azo}}$-1Co$\mathbf{L_H}$-1Fe$\mathbf{T_{Fc}}$] (($\mathbf{A_{azo}}$)$_2$ = bis((4-(4′-2,2′;6′,2″-terpyridyl)phenylazo)phenyl)disulfide, $\mathbf{L_H}$ = bis(terpyridyl)-*p*-phenylene), displayed a rate constant, k_{et}, for electron transfer at the terminal Fc moiety that was twice that obtained from wires prepared in the sequence electrode-$Fe(tpy)_2$-$Co(tpy)_2$-Fc, Au-[$\mathbf{A_{azo}}$-1Fe$\mathbf{L_H}$-1Co$\mathbf{T_{Fc}}$]. This suggested that the oxidation reaction at the terminal Fc moiety was mediated by electron transfer via $Co(tpy)_2$ more efficiently than via $Fe(tpy)_2$. Metal complex wires with an inherent potential gradient based on the heteroligand combination were synthesized using bis(4-(4′-2,2′;6′,2″-terpyridyl) phenyl)disulfide, ($\mathbf{A_H}$)$_2$, or bis(4-(4′-5,5″-difluoro-2,2′;6′,2″-terpyridyl)phenyl)disulfide, ($\mathbf{A_F}$)$_2$, as anchoring ligands and bis(terpyridyl)-*p*-phenylene, L_H, or bis(terpyridyl)-tetrafluoro-*p*-phenylene, $\mathbf{L_F}$, as bridging ligands. Potential step chronoamperometry (PSCA) measurements of the redox reaction of Au-[$\mathbf{A_H}$-1Fe$\mathbf{L_1}$-2Fe$\mathbf{L_F}$] and Au-[$\mathbf{A_F}$-1Fe$\mathbf{L_F}$-2Fe$\mathbf{L_H}$] revealed only small differences in the current–time curves, indicating that the electron self-exchange between the $Fe(tpy)_2$ units in a wire was faster than electron transfer between an electrode surface and the adjacent $Fe(tpy)_2$ units. Fast electron self-exchange suppressed the expected rectification behavior of the wire, despite the presence of a potential staircase within the wire.

Keywords: coordination programming; cyclic voltammogram; electrochemistry; potential gradient; terpyridine complex

Introduction

"Coordination programming" utilizes the advantages of coordination chemistry to control the chemical bonds and arrangements of metal atoms and ions for the creation of superstructures, particularly for the construction of molecular wires on surfaces. Coordination programming involves designing methods for immobilizing and assembling molecular wires on electrodes in a controlled manner with the goal of constructing designed molecular networks. Coordination programming is, therefore, an important fundamental issue in the development of molecular electronics.[1] We recently reported the construction of one- and three-dimensional redox complex oligomer wires on gold,[2–7] ITO,[8,9] and silicon surfaces.[10] This method involved creating stepwise alternating connections between rigid bis- or tri-

Department of Chemistry, School of Science, The University of Tokyo, Tokyo 113-0033, Japan
E-mail: nisihara@chem.s.u-tokyo.ac.jp

(terpyridine) bridging ligands and octahedral metal ions to provide, respectively, linear or branched oligomer wires with a desired number and sequence of metal complex units.[4,10] The electron transport mechanism and redox reaction kinetics of the films composed of linear and branched oligomer wires were examined, yielding the first observation of redox conduction through a single molecular wire in a redox polymer film.[4] We also found that the π-conjugated bis(terpyridine)metal, $M(tpy)_2$, oligomer wires showed superior long-range electron transport capabilities. The attenuation factor, β^d, indicated the degree of reduction in the logarithm of the electron transfer rate constant as a function of distance along the molecular wire between the electrode and the redox-active species at the terminus of the wire. The attenuation factors were found to be 0.008–0.07 $Å^{-1}$ and 0.002–0.004 $Å^{-1}$ for molecular wires composed of $Fe(tpy)_2$ and $Co(tpy)_2$ oligomers, respectively.[6] The stepwise coordination method was used to construct a system that could clarify how the electron transport behavior of molecular wires depended on the surface junctions at the molecular level by changing only the surface-anchoring molecular unit. The dependence of the electron transfer rate constant, k_{et}, and the electron transport abilities of $Fe(tpy)_2$ oligomer wires on three surface-anchoring tpy ligands indicated a significant difference between the k_{et} values due to the electronic and steric properties of the surface-anchoring ligands. The three anchoring ligands provided comparable β^d values.[7]

The next stage of the research involved introducing an inherent potential gradient over the molecular wire. The presence of potential steps can control the direction of electron transfer to enable almost perfectly efficient photo-electron conversion in photosystems I and II of the light reaction during photosynthesis.[11] Potential junctions have also been studied toward development of molecular rectifiers.[12]

In this research, we aimed to develop metal complex oligomer wires prepared via a stepwise coordination method using multiple metal ions (Fe, Co) and ligands (Figure 1) in a single molecular wire. As a first step, we prepared heterometal complex oligomer wires and measured their electrochemical behavior. Next, we fabricated complex oligomer wires with an inherent potential staircase using heteroligand combinations. Differences between the electron transfer behaviors of these heterometal complex structures and the homo structures, in terms of the potential gradient and/or irregularities, were examined using electrochemical methods.

Experimental Part

Materials

Bis((4-(4′-2,2′;6′,2″-terpyridyl)phenylazo)-phenyl)disulfide ($(\mathbf{A_{azo}})_2$),[3] bis(4-(4′-2,2′;6′,2″-terpyridyl)phenyl)disulfide, ($(\mathbf{A_H})_2$),[4] $Pd(PPh_3)_4$,[13] $\mathbf{T_{Fc}}$,[14] and 4′-(4-anilino)-2,2′:6′,2″-terpyridine[15] were prepared according to the methods described in the literature. Other compounds were obtained from commercial sources.

Synthesis

2-Acetyl-5-Fluoropyridine

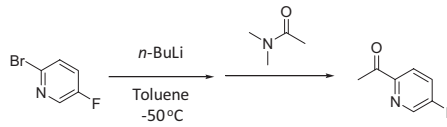

Under a nitrogen atmosphere, 1.65 M *n*-butyllithium (14 mL, 23.1 mmol) was added to a stirred solution of 2-bromo-5-fluoropyridine (3.55 g, 20.2 mmol) in dry toluene (150 mL) at −50 °C. After stirring for 1 h, dehydrated *N*, *N*-dimethylacetamide (2.0 mL, 21.6 mmol) was added to the reaction mixture. The solution was then allowed to warm to room temperature. Stirring continued for 1 h, and a saturated solution of NH_4Cl aq was added to the reaction solution to quench the reaction. The reaction solution was extracted with toluene, and the toluene layer was dried

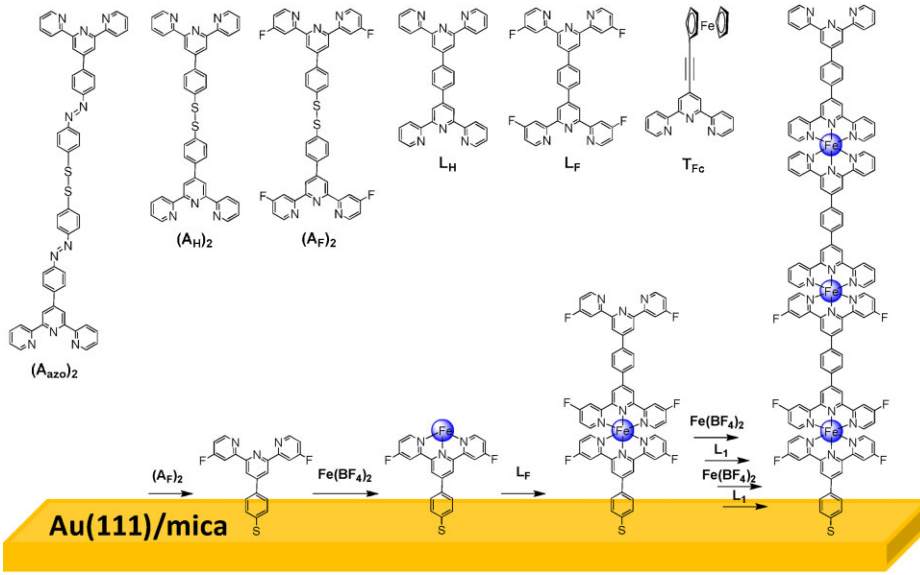

Figure 1.
Chemical structures of the ligands and surface coordination programming of the metal complex oligomer wires.

over Na_2SO_4. After removing the solvent, the residue was purified by silica column chromatography, eluted with hexane/ethyl acetate (4:1 v/v). The product was obtained as a colorless solid. Yield: 1.63 g (11.7 mmol, 58%). ^{1}H NMR ($CDCl_3$, 400 MHz) δ: 8.51 (d, $J = 2.5$ Hz, 1H), 8.11 (dd, $J = 4.6$, 8.4 Hz, 1H), 7.52 (dt, $J = 2.5$, 8.4 Hz, 2H), 2.71 (s, 3H). ^{13}C NMR ($CDCl_3$, 100 MHz) δ: 198.40, 161.44 (d, $J = 261.9$ Hz), 150.18 (d, $J = 4.2$ Hz), 137.32 (d, $J = 24.8$ Hz), 123.63 (d, $J = 5.8$ Hz), 123.37 (d, $J = 18.2$ Hz), 25.68. EI-MS: $m/z = 139$ $[M]^+$, calcd for C_7H_6FNO, 139. Anal. Calcd for C_7H_6FNO: C, 60.43; H, 4.35; N, 10.07. Found: C, 60.47; H, 4.08; N, 10.17.

1,4-Bis(4′-(4′-5,5″-Difluoro-2,2′;6′,2″-Terpyridyl))-Benzene (L_F)

Terephthalaldehyde (0.220 g, 1.64 mmol), 2-acetyl-5-fluoropyridine (1.014 g, 7.29 mmol), and potassium hydroxide (0.640 g, 11.2 mmol) were dissolved in a mixture of EtOH (20 mL) and 28% NH_3 aq (10 mL). The mixture was stirred for 23 h at 50 °C. The solid residue obtained by filtering, and the reaction mixture was washed with EtOH. The product was obtained by recrystallization from pyridine as a colorless solid. Yield: 0.167 g (0.273 mmol, 17%). ^{1}H NMR ($CDCl_3$, 400 MHz) δ: 8.74 (s, 2H), 8.70 (dd, $J = 4.9$, 8.8 Hz, 2H), 8.60 (d, $J = 2.8$ Hz, 2H), 8.05 (s, 2H), 7.61 (dt, $J = 2.8$, 8.4 Hz, 2H). ESI-TOF-MS: $m/z = 613.17$ $[M + H]^+$, calcd for M + H, 613.27. Anal. Calcd for $C_{36}H_{20}N_6F_4$: C, 70.58; H, 3.29; N, 13.72. Found: C, 70.58; H, 3.50; N, 13.53.

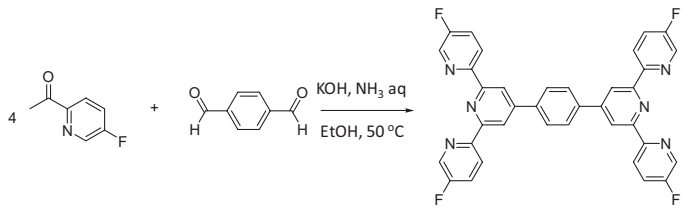

1-Nitro-4-(4′-5,5″-Difluoro-2,2′;6′,2″-Terpyridyl)-Benzene (tpyPhNO$_2$-F$_2$)

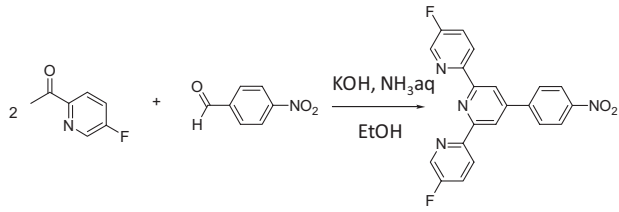

2-Acetyl-5-fluoropyridine (0.756 g, 5.43 mmol), 4-nitro-benzaldehyde (0.409 g, 2.71 mmol), and potassium hydroxide (0.320 g, 5.38 mmol) were dissolved in a mixture of EtOH (15 mL) and 28% NH_3 aq (3 mL). The solution was stirred for 48 h. A precipitate was obtained by filtering the reaction mixture. The precipitate was then washed with EtOH and MeOH. The residue was chromatographed on an alumina gel column and eluted with CH_2Cl_2, followed by separation on a silica gel column and elution with chloroform, to afford the product. Yield: 0.200 g (0.512 mmol, 19%). ^{1}H NMR ($CDCl_3$, 400 MHz) δ: 8.71–8.64 (m, 4H), 8.58 (d, $J = 3.0$ Hz, 2H), 8.39 (d, $J = 8.5$ Hz, 2H), 8.04 (d, $J = 8.3$ Hz, 2H), 7.61 (dt, $J = 3.0$, 8.3 Hz, 2H). ^{13}C NMR ($CDCl_3$, 100 MHz) δ: 160.12 (d, $J = 257.5$ Hz), 155.45, 151.86 (d, $J = 4.8$ Hz), 148.25, 148.07, 144.81, 137.45 (d, $J = 23.9$ Hz), 128.27, 124.27, 123.73 (d, $J = 18.1$ Hz), 122.60 (d, $J = 4.8$ Hz), 118.66. MALDI-TOF-MS: $m/z = 390.10$ $[M + H]^+$, calcd for M + H, 390.97. Anal. Calcd for $C_{21}H_{12}N_4O_2F_2$: C, 64.62; H, 3.10; N, 14.35. Found: C, 64.65; H, 3.35; N, 14.11.

1-Amino-4-(4′-5,5″-Difluoro-2,2′;6′,2″-Terpyridyl)-Benzene (tpyPhNH$_2$-F$_2$)

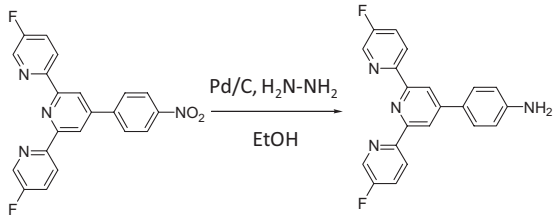

Under a nitrogen atmosphere, ethanol (100 mL) was added to tpyPhNO$_2$-F$_2$ (0.179 g, 0.459 mmol) and 5% Pd/C (0.192 g). Hydrazine monohydrate (1 mL, 20.6 mmol) was added to the mixture. After refluxing for 2 h, the palladium catalyst was removed by filtration, and the catalyst was washed with CH_2Cl_2. After removing the solvent, the residue was dissolved in CH_2Cl_2, and the organic layer was washed with water and dried over Na_2SO_4. The product was obtained by evaporating the solvent, yielding as pale yellow powder. Yield: 0.138 g (0.383 mmol, 83%). ^{1}H NMR ($CDCl_3$, 400 MHz) δ: 8.65 (dd, $J = 4.6$, 8.8 Hz, 2H), 8.61 (s, 2H), 8.56 (d, $J = 2.9$ Hz, Hz, 2H), 7.56 (dt, $J = 2.8$, 8.4 Hz, 2H), 6.81 (d, $J = 8.4$ Hz, 2H), 3.89 (br, 2H). ^{13}C NMR ($CDCl_3$, 100 MHz) δ: 159.69 (d, $J = 256.5$ Hz), 154.81, 152.73 (d, $J = 3.8$ Hz), , 150.13, 147.63, 137.19 (d, $J = 23.8$ Hz), 128.33, 128.01, 123.52 (d, $J = 18.1$ Hz), 122.46 (d, $J = 4.8$ Hz), 117.46, 115.23. MALDI-TOF-MS: $m/z = 361.13$ $[M + H]^+$, calcd for M + H, 361.02. HR-MS(ESI-TOF-MS) calcd for $C_{21}H_{14}F_2N_4Na$, 383.1084; found 383.1038 ($[M + Na]^+$).

Bis(4-(4′-5,5″-Difluoro-2,2′;6′,2″-Terpyridyl)-Phenyl)disulfide, ($(A_F)_2$)

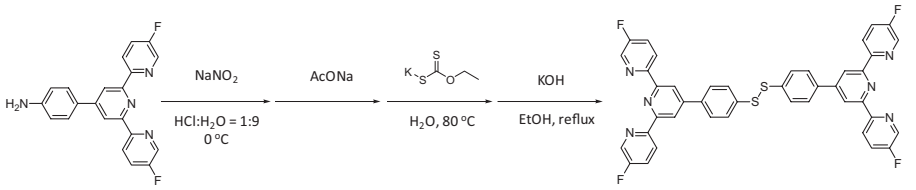

tpyPhNH$_2$-F$_2$ (0.187 g, 0.519 mmol) was dissolved in a 25 mL solution containing hydrochloric acid and water in a ratio of 1:9. Sodium nitrite (0.182 g, 2.64 mmol) in 1 mL of water was added dropwise to the solution at 0 °C. The reaction mixture was stirred for 1 h at 0 °C. Sodium acetate (3.793 g, 46.1 mmol) was slowly added to the diazonium solution in order to deacidify the solution to a pH of 4. The diazonium solution was then added, over 10 min, to a stirred solution of potassium ethyl xanthate (3.805 g, 21.4 mmol) in 5 mL of water heated to 60 °C. The mixture was heated for an additional 30 min, then cooled. The mixture was extracted with chloroform. The extracts were washed with 10% NaOH aq and twice with water. After removing the solvent, 80 mL ethanol and potassium hydroxide (1.470 g, 22.4 mmol) were added, and the mixture was heated to reflux for 1 h. The reaction was then quenched by adding a saturated solution of NH_4Cl aq. The reaction mixture was evaporated to remove the ethanol. The residue was extracted with chloroform, and the chloroform layer was dried over Na_2SO_4. After the solvent had been removed, the residue was purified by alumina column chromatography and eluted with chloroform. The solvent was evaporated, and the product was obtained as a colorless powder. Yield: 0.115 g (0.153 mmol, 59%). ^{1}H NMR ($CDCl_3$, 400 MHz) δ: 8.67–8.65 (m, 4H), 8.55 (d, $J = 2.7$ Hz, 2H), 7.85 (d, $J = 8.3$ Hz, 2H), 7.68 (d, $J = 8.3$ Hz, 2H), 7.57 (dt, $J = 2.9$, 8.4 Hz, 2H). ^{13}C NMR ($CDCl_3$, 100 MHz) δ: 159.75 (d, $J = 256.5$ Hz), 155.10, 152.30 (d, $J = 4.8$ Hz), 149.42, 138.03, 137.41, 137.30 (d, $J = 22.9$ Hz), 127.99, 127.97, 123.57 (d, $J = 18.1$ Hz), 122.47 (d, $J = 4.7$ Hz), 118.33. MALDI-TOF-MS: $m/z = 753.20$ $[M + H]^+$, calcd for $C_{42}H_{25}F_4N_6S_2$, 753.15. HR-MS (ESI-TOF-MS) calcd for $C_{42}H_{25}F_4N_6S_2$, 753.1519; found 753.1510 ($[M + H]^+$).

Method for Preparing the Complex Oligomer Wires

The complex wires used in this study, [$\mathbf{A_{azo}}$-$\mathbf{1Fe L_1}$-$\mathbf{1CoT_{Fc}}$], [$\mathbf{A_{azo}}$-$\mathbf{1CoL_1}$-$\mathbf{1FeT_{Fc}}$], [$\mathbf{A_H}$-$\mathbf{1FeL_H}$-$\mathbf{2FeL_F}$], [$\mathbf{A_F}$-$\mathbf{1FeL_F}$-$\mathbf{2FeL_H}$], and [$\mathbf{A_H}$-$\mathbf{1FeL_H}$] were prepared by a method that was the same or analogous to methods described in the literature.[4,6] A typical procedure is as follows (see Figure 1); a film of [$\mathbf{A_F}$-$\mathbf{1FeL_{F4}}$-$\mathbf{2FeL_1}$] was prepared by immersing an Au/mica plate in a solution of phenyl disulfide (1 mM) in chloroform for 5 h, followed by rinsing with chloroform and drying with nitrogen gas. The surface was covered sparsely with tpy-terminated molecules by immersing the plate in a solution of $(\mathbf{A_F})_2$ (0.1 mM) for 3 h. The plate was then immersed in an ethanol solution of $Fe(BF_4)_2$ (0.1 M) for 1 h, washed with water and ethanol, and dried. The plate was immersed in a chloroform solution of $\mathbf{L_F}$ for 15 h, washed with chloroform, and dried. The plate was then immersed alternately in an ethanol solution of $Fe(BF_4)_2$ (0.1 M) and a solution of $\mathbf{L_H}$ (0.1 mM) in chloroform, with the corresponding washing and drying processes for each cycle.

Electrochemical Measurements

Electrochemical measurements were carried out using an Au/mica working electrode (electrode area: 0.264 cm^2) covered by a metal complex film, a Pt-wire counter electrode, and an Ag^+/Ag reference electrode ($AgClO_4$ (0.01 M) in Bu_4NClO_4-MeCN (0.1 M)) in a standard one-compartment cell. Cyclic voltammetry and potential

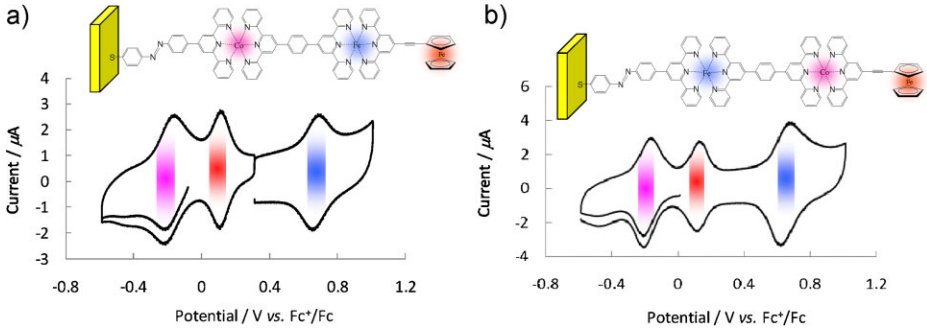

Figure 2.
Cyclic voltammograms of [$\mathbf{A_{azo}}$-**1CoL$_H$-1FeT$_{Fc}$**] (a) and [$\mathbf{A_{azo}}$-**1FeL$_H$-1CoT$_{Fc}$**] (b) in 1 M Bu_4NClO_4-CH_2Cl_2 at a scan rate of 0.1 Vs^{-1}.

step chronoamperometry (PSCA) were performed using an ALS 750A or ALS 650B electrochemical analyzer. All experiments were carried out under argon at 25 °C.

Results and Discussion

Electron Transfer Behavior Through the Heterometal Complex Wires

Ferrocene-terminated heterometal complex wires, [$\mathbf{A_{azo}}$-**1FeL$_1$-1CoT$_{Fc}$**] and [$\mathbf{A_{azo}}$-**1CoL$_1$-1FeT$_{Fc}$**], were prepared on a gold surface via stepwise coordination reactions (Figure 1). The cyclic voltammograms of the wires are shown in Figure 2a and 2b, respectively. Although overlap of the two redox peaks corresponding to the $Fc^{+/0}$ and $Co(tpy)_2^{3+/2+}$ couples prevented us from accurately estimating the surface coverage of the Fc^+/Fc and $Co(tpy)_2^{3+/2+}$ couples independently, the ratio of the areas of the redox peaks corresponding to the $Fc^{+/0}$, $Co(tpy)_2^{3+/2+}$, and $Fe(tpy)_2^{3+/2+}$ couples was approximately 1:1:1, as expected. The redox potentials of $Co(tpy)_2^{3+2+}$, $Fc^{+/0}$, and $Co(tpy)_2^{3+2+}$ did not vary with the metal ion sequence in the wire, according to the cyclic voltammograms (–0.20 V, 0.11 V, and 0.67 V for [$\mathbf{A_{azo}}$-**1CoL$_H$-1FeT$_{Fc}$**], and –0.19 V, 0.12 V, and 0.65 V for [$\mathbf{A_{azo}}$-**1FeL$_H$-1CoT$_{Fc}$**], respectively). This results suggested that the electronic interaction between Fc and $Co(tpy)_2$ or $Fe(tpy)_2$ was not strong.

The electron transfer behavior at the Fc moiety in the heterometal complex wires was investigated using PSCA with a potential step from –0.01 V, approximately midway between the potentials of Fc and $Co(tpy)_2$, to a potential of 0.16–0.51 V. This potential step permitted observation of the redox current corresponding to the Fc moiety only in the cases of [$\mathbf{A_{azo}}$-**1FeL$_H$-1CoT$_{Fc}$**] and [$\mathbf{A_{azo}}$-**1CoL$_H$-1FeT$_{Fc}$**]. The electron transfer rate constants, k_{et}, estimated from the PSCA results are shown in Figure 3. If the decay of the electron transfer kinetics through heterometal wire agrees with the sum of the decays derived

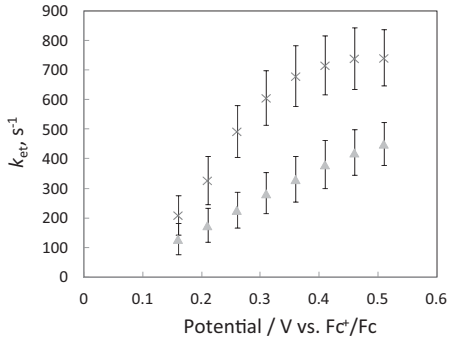

Figure 3.
Dependence of the electron transfer kinetics at the Fc moiety within [$\mathbf{A_{azo}}$-**1CoL$_H$-1FeT$_{Fc}$**] (×) and [$\mathbf{A_{azo}}$-**1FeL$_H$-1CoT$_{Fc}$**] (▲) and wires on the electrode potential, in 1 M Bu_4NClO_4-CH_2Cl_2.

from the iron and cobalt complexes in homogeneous wires, studied previously,[4] then the electron transfer kinetics of the terminal ferrocene in [$\mathbf{A_{azo}}$-$\mathbf{1FeL_H}$-$\mathbf{1CoT_{Fc}}$] and in [$\mathbf{A_{azo}}$-$\mathbf{1CoL_H}$-$\mathbf{1FeT_{Fc}}$] should be the same; however, these rate constants in [$\mathbf{A_{azo}}$-$\mathbf{1CoL_H}$-$\mathbf{1FeT_{Fc}}$] were about twice the rate constants in [$\mathbf{A_{azo}}$-$\mathbf{1FeL_H}$-$\mathbf{1CoT_{Fc}}$]. This observation could be understood in the event that the oxidation reaction at the terminal Fc moiety was more efficiently mediated by electron transfer to $Co(tpy)_2$ than to $Fe(tpy)_2$ because the phenylene-linked $Co(tpy)_2$ oligomer wire had a β^d of 0.004, whereas the phenylene-linked $Fe(tpy)_2$ oligomer wire had a β^d of 0.02. Under this hypothesis, an electron charge initially migrated from Fc to $Co(tpy)_2$ within the wire, followed by transfer to the electrode. Charge transfer from the Fc moiety to the cobalt complex moiety in the wire that yielded faster electron transfer, [$\mathbf{A_{azo}}$-$\mathbf{1CoL_H}$-$\mathbf{1FeT_{Fc}}$], would, therefore, be slower than in the [$\mathbf{A_{azo}}$-$\mathbf{1FeL_H}$-$\mathbf{1CoT_{Fc}}$] wire because the distance between the ferrocene and the cobalt complex moiety in the former was longer than in the latter; however, back electron transfer in the former was also slow. As a result, the charge on the cobalt complex moiety preferred to migrate toward the electrode. The concept that electron and hole separation prevents charge recombination is generally applicable in studies of long-lived charge-separated states.[16] Here, surprisingly, the relatively short distance between the Fc and cobalt complex moieties and the long distance between the cobalt complex moiety and the electrode in [$\mathbf{A_{azo}}$-$\mathbf{1FeL_H}$-$\mathbf{1CoT_{Fc}}$] produced a slower overall electron transfer.

Although the electron transfer mechanism within heterometal complex wires cannot be understood through a simple explanation based on these results, the fact that the electron transfer properties of the complex wires could be controlled via the linear sequence of metal ions over the complex wire is intriguing. This fact indicates that heterometal alignment within

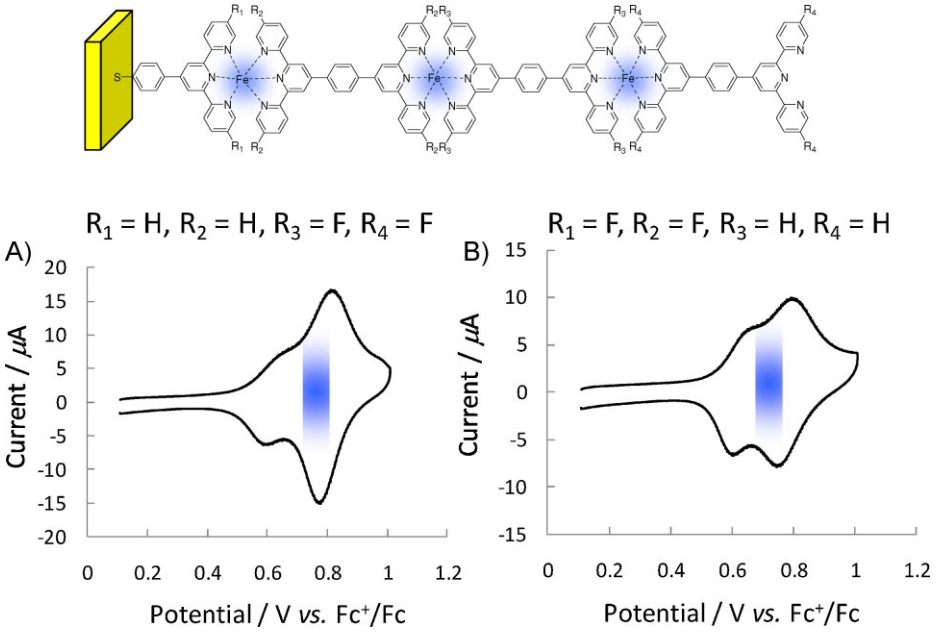

Figure 4.
Cyclic voltammograms of [$\mathbf{A_H}$-$\mathbf{1FeL_H}$-$\mathbf{2FeL_F}$] (**A**) and [$\mathbf{A_F}$-$\mathbf{1FeL_F}$-$\mathbf{2FeL_H}$] (**B**) in 1 M Bu_4NClO_4-CH_2Cl_2 at a scan rate of 0.1 Vs^{-1}.

metal complex wires can potentially be used to fabricate complex wires with a wide variety of properties by employing a range of metal ions.

Electron Transfer Through $Fe(tpy)_2$ Oligomer Wires with an Inherent Potential Gradient

In the field of molecular electronics, it is highly desirable to engineer molecular systems that achieve specific functions. Rectification behavior in a single molecular wire is particularly an attractive device function. Here, we attempted to construct complex wires with an inherent potential staircase to achieve rectification behavior. To simplify the wire system, a single *p*-phenylene moiety was used for the bridging ligands, and L_H and the fluorinated ligand $\mathbf{L_F}$ were used to construct the complex wires. The redox potential of the bis(terpyridine)iron complex shifted toward positive values upon introduction of fluorinated terpyridine, from 0.63 V to 0.80 V *vs.* Fc^+/Fc. The electronic properties of the wires with an inherent potential staircase were

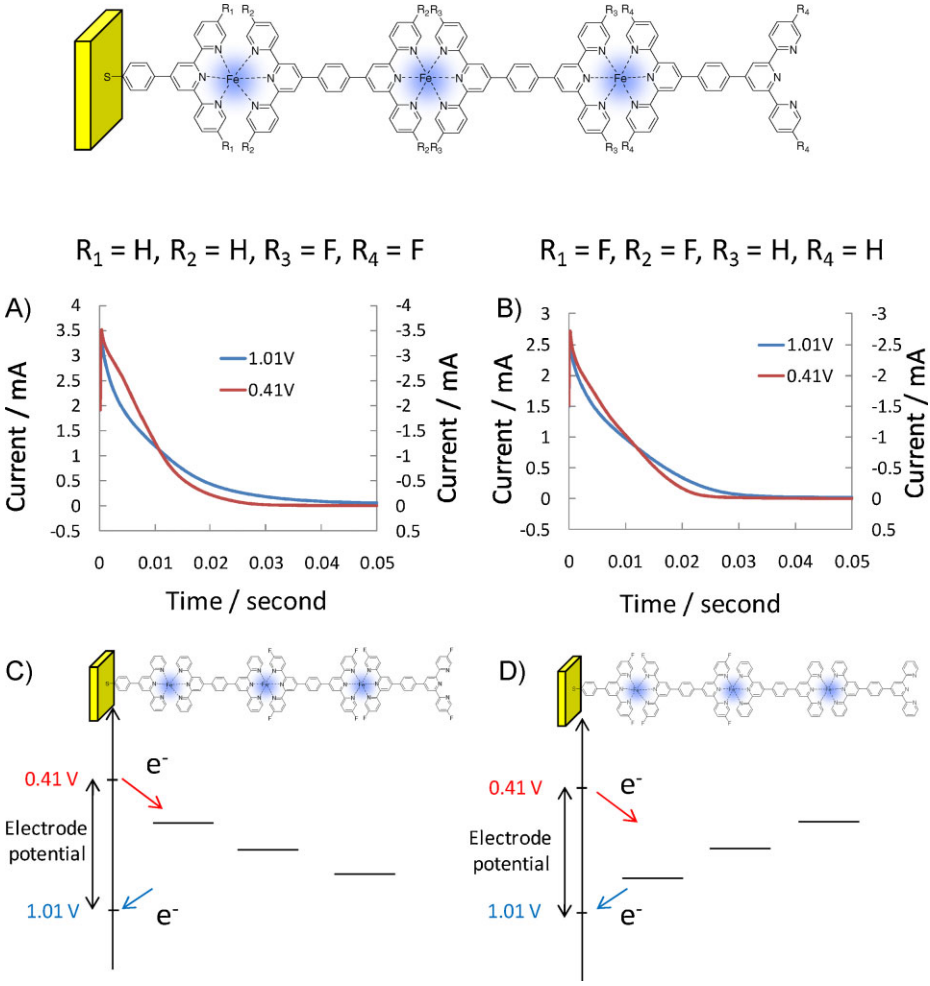

Figure 5.
Chronoamperograms of [$\mathbf{A_H}$-1Fe$\mathbf{L_H}$-2Fe$\mathbf{L_F}$] at electrode potentials of 1.01 V (left axis) and 0.41 V (right axis) (A), and [$\mathbf{A_F}$-1Fe$\mathbf{L_F}$-2Fe$\mathbf{L_H}$] at electrode potentials of 1.01 V (left axis) and 0.41 V (right axis) (B). Schematic diagram of the redox potential of the iron complexes within the wires, [$\mathbf{A_H}$-1Fe$\mathbf{L_H}$-2Fe$\mathbf{L_F}$] (C), [$\mathbf{A_F}$-1Fe$\mathbf{L_F}$-2Fe$\mathbf{L_H}$] (D).

evaluated by preparing [$\mathbf{A_H}$-1Fe$\mathbf{L_H}$-2Fe$\mathbf{L_F}$] and [$\mathbf{A_F}$-1Fe$\mathbf{L_F}$-2Fe$\mathbf{L_H}$]. Cyclic voltammograms of the wires are shown in Figure 4. Overlapping peaks were observed over the range 0.6 V to 0.8 V *vs.* Fc^+/Fc, consistent with the redox potentials of iron complexes of terpyridine and fluorinated terpyridine; therefore, these wires displayed an inherent potential gradient.

The electron transport properties of the wires were evaluated by applying a potential step that was intermediated between the potentials at which the iron complexes within the wire could be virtually reduced and oxidized, 0.41 V and 1.01 V, respectively. The resulting chronoamperograms, shown in Figure 5, revealed that the reduction current was larger than the oxidation current, as expected from the redox potential sequence for [$\mathbf{A_H}$-1Fe$\mathbf{L_H}$-2Fe$\mathbf{L_F}$]; however, the [$\mathbf{A_F}$-1Fe$\mathbf{L_F}$-2Fe$\mathbf{L_H}$] wire, which was prepared to have an inverted sequence of redox potentials relative to the former wire, displayed a reduction current that was slightly larger than the oxidation current. Obvious rectification behavior was not observed because the rate-determining step of the redox reaction along the wire was electron transfer between the electrode and the complex directly attached to the electrode, as reported previously.[4,7] Additionally, the dependence of the electron transfer kinetics between the electrode and the complex attached to the electrode on the electrode potential, as shown in Figure 6, indicated that the reduction reaction was faster than the oxidation reaction at the same absolute overpotential. Therefore, we concluded that fast self-exchange between $Fe(tpy)_2$ units in a wire suppressed the expected rectification behavior of the wire, despite the presence of an inherent potential staircase within the wire. To realize rectification behavior, other surface-attachment ligands must be used such that the electron transfer kinetics between the electrode and the complex exceed the self-exchange kinetics between the complexes within the wire. Alternatively, it may be sufficient to modify the ligands in such a way as to magnify the redox potential difference.

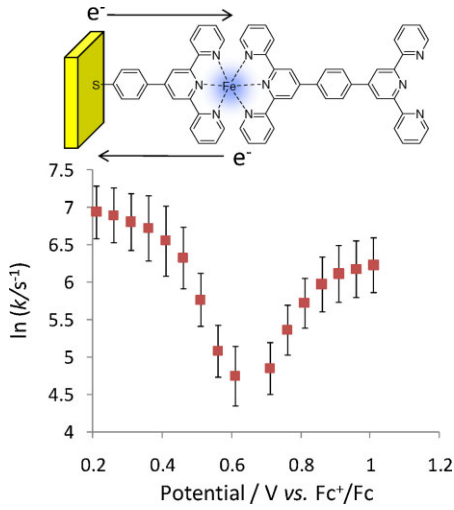

Figure 6.
The dependence of the electron transfer rate constants at the iron complex within [$\mathbf{A_H}$-1Fe$\mathbf{L_H}$] on the electrode potential, in 1 M Bu_4NClO_4-CH_2Cl_2.

Conclusion

π-Conjugated $M(tpy)_2$ oligomer wires with an inherent potential gradient were prepared using a combination of metals and bridging ligands. The electron transfer and transport behaviors were analyzed electrochemically. The heterometal complex wire [$\mathbf{A_{azo}}$-1Co$\mathbf{L_H}$-1Fe$\mathbf{T_{Fc}}$] showed a larger rate constant, k_{et}, for electron transfer at the terminal Fc moiety than was observed in [$\mathbf{A_{azo}}$-1Fe$\mathbf{L_H}$-1Co$\mathbf{T_{Fc}}$]. This difference was not large but it suggested that the oxidation reaction at the terminal Fc moiety was more efficiently mediated by electron transfer to $Co(tpy)_2$ than to $Fe(tpy)_2$. Cyclic voltammograms of the metal complex wires with heteroligand combinations, [$\mathbf{A_H}$-1Fe$\mathbf{L_1}$-2Fe$\mathbf{L_F}$] and [$\mathbf{A_F}$-1Fe$\mathbf{L_F}$-2Fe$\mathbf{L_H}$], indicated the formation of an inherent potential gradient; however, the redox conduction behaviors revealed by PSCA were not significantly different probably due to the slow electron transfer

kinetics at the electrode–molecular wire junction. These results indicated that the π-conjugated metal complex wires were good electron transporters. The introduction of resistive moieties into the wires is necessary to control the direction and rate of electron transport more effectively.

Acknowledgements: The authors acknowledge Grants-in-Aid from MEXT of Japan (Nos. 20245013 and 21108002, area 2107, Coordination Programming) and the Global COE Program for Chemistry Innovation for financial support.

[1] (a) Y. Yamanoi, H. Nishihara, *Chem. Commun.* **2007**, *3983*; (b) H. Nishihara, K. Kanaizuka, Y. Nishimori, Y. Yamanoi, *Coord. Chem. Rev.* **2007**, *251*, 2674; (c) Y. Nishimori, Y. Yamanoi, S. Kume, H. Nishihara, *Electrochemistry*, **2007**, *75*, 770; (d) M. Miyachi, H. Nishihara, in: "*Macromolecules Containing Metal and Metal-Like Elements*", *Vol.* 10, A. S., Abd-El-Aziz, C. E., Carraher, P. D., Harvey, C. U., Pittman, M. Zeldin, Eds., Wiley, **2010**, Chapter 11, pp. 387–3414.

[2] K. Kanaizuka, M. Murata, Y. Nishimori, I. Mori, K. Nishio, H. Masuda, H. Nishihara, *Chem. Lett.* **2005**, *34*, 534.

[3] Y. Ohba, K. Kanaizuka, M. Murata, H. Nishihara, *Macromol. Symp.* **2006**, *235*, 31.

[4] Y. Nishimori, K. Kanaizuka, M. Murata, H. Nishihara, *Chem. Asian J.* **2007**, *2*, 367.

[5] M. Utsuno, F. Toshimitsu, S. Kume, H. Nishihara, *Macromol. Symp.* **2008**, *270*, 153.

[6] Y. Nishimori, K. Kanaizuka, T. Kurita, T. Nagatsu, Y. Segawa, F. Toshimitsu, S. Muratsugu, M. Utsuno, S. Kume, M. Murata, H. Nishihara, *Chem. Asian J.* **2009**, *4*, 1361.

[7] T. Kurita, Y. Nishimori, F. Toshimitsu, S. Muratsugu, S. Kume, H. Nishihara, *J. Am. Chem. Soc.* **2010**, *132*, 4524.

[8] M. Miyachi, M. Ohta, M. Nakai, Y. Kubota, Y. Yamanoi, T. Yonezawa, H. Nishihara, *Chem. Lett.* **2008**, *37*, 404.

[9] M. Miyachi, Y. Yamanoi, T. Yonezawa, H. Nishihara, M. Iwai, M. Konno, M. Iwai, Y. Inoue, *J. Naosci. Nanotech.* **2009**, *9*, 1722.

[10] H. Maeda, R. Sakamoto, Y. Nishimori, J. Sendo, F. Toshimitsu, Y. Yamanoi, H. Nishihara, *Chem. Commun.* **2011**, *47*, 8644.

[11] S. I. Allakhverdiev, V. Thavasi, V. D. Kreslavski, S. K. Zharmukhamedov, V. V. Klimov, S. Ramakrishna, D. A. Los, M. Mimuro, H. Nishihara, R. Carpentier, *J. Photochem. Photobiol., C: Photochem. Rev.* **2010**, *11*, 101.

[12] (a) I. Díez-Pérez1, J. Hihath, Y. Lee, L. Yu, L. Adamska, M. A. Kozhushner, I. I. Oleynik, N. Tao, *Nature Chem.* **2009**, *1*, 635; (b) M. L. Chabinyc, X. Chen, R. E. Holmlin, H. H. Jacobs, H. Skulason, C. D. Frisbie, V. Mujica, M. A. Ratner, M. A. Rampi, G. M. Whitesides, *J. Am. Chem. Soc.* **2002**, *124*, 11730; (c) M. Elbing, R. Ochs, M. Koentopp, M. Fischer, C. von Hänisch, F. Weigend, F. Evers, H. B. Weber, M. Mayor, *Proc. Natl Acad. Sci. USA* **2005**, *102*, 8815; (d) R. H. M. Smit, Y. Noat, C. Untiedt, N. D. Lang, M. C. van Hemert, J. M. van Ruitenbeek, *Nature* **2002**, *419*, 906.

[13] D. R. Coulson, *Inorg. Synth.* **1973**, *13*, 121.

[14] U. Siemeling, J. Vor der Brüggen, U. Vorfeld, B. Neumann, A. Stammler, H.-G. Stammler, A. Brockhinke, R. Plessow, P. Zanello, F. Laschi, F. F. de Biani, M. Fontani, S. Stanseenken, M. Stapper, G. Gurzadyan, *Chem. Eur. J.* **2003**, *9*, 2819–2833.

[15] J. R. Peterson, T. A. Smith, P. Thordarson, *Chem. Commun.* **2007**, *19*, 1899.

[16] H. Imahori, D. M. Guldi, K. Tamaki, Y. Yoshida, C. Luo, Y. Sakata, S. Fukuzumi, *J. Am. Chem. Soc.* **2001**, *123*, 6617.

